

Pitfalls of FDG-PET for the diagnosis of osteoblastic bone metastases in patients with breast cancer

Takako Nakai^{1,3}, Chio Okuyama¹, Takao Kubota¹, Kei Yamada¹, Yo Ushijima¹, Keiko Taniike², Takako Suzuki², Tsunehiko Nishimura¹

¹ Department of Radiology, Graduate School of Medical Science, Kyoto Prefectural University of Medicine Kyoto, Japan

² Nishijin Hospital Kyoto, Japan

³ Department of Radiology, Kyoto Prefectural University of Medicine, 465 Kajicho Kawaramachi-Hirokouji Kamigyō Kyoto Kyoto, 602-8566, Japan

Received: 23 March 2005 / Accepted: 29 April 2005 / Published online: 20 August 2005

© Springer-Verlag 2005

Abstract. *Purpose:* The purpose of this study was to investigate the pitfalls of using 2-[¹⁸F]-fluoro-2-deoxy-D-glucose positron emission tomography (FDG-PET) for the evaluation of osteoblastic bone metastases in patients with breast cancer by comparing it with ^{99m}Tc-hydroxymethylene diphosphonate bone scintigraphy.

Methods: Among the 89 breast cancer patients (mean age 59±15 years) who had undergone both FDG-PET and bone scintigraphy within 1 month between September 2003 and December 2004, 55 with bone metastases were studied. The bone metastases were visually classified by multi-slice CT into four types according to their degree of osteosclerosis and osteolysis—osteoblastic, osteolytic, mixed and invisible—and compared in terms of tracer uptake on FDG-PET or bone scintigraphy and SUV_{mean} on FDG-PET. Differences in the rate of detection on bone scintigraphy and FDG-PET were analysed for significance by the McNemar test.

Results: The sensitivity, specificity and accuracy of bone scintigraphy were 78.2%, 82.4% and 79.8% respectively, and those of FDG-PET were 80.0%, 88.2% and 83.1%, respectively, revealing no significant differences. According to the CT image type, the visualisation rate of bone scintigraphy/FDG-PET was 100%/55.6% for the blastic type, 70.0%/100.0% for the lytic type, 84.2%/94.7% for the mixed type and 25.0%/87.5% for the invisible type. The visualisation rates of bone scintigraphy for the blastic type and FDG-PET for the invisible type were significantly higher. The SUV_{mean} of the blastic, lytic, mixed and invisible types were 1.72±0.28, 4.14±2.20,

2.97±1.98 and 2.25±0.80, respectively, showing that the SUV_{mean} tended to be higher for the lytic type than for the blastic type.

Conclusion: FDG-PET showed a low visualisation rate in respect of osteoblastic bone metastases. Although FDG-PET is useful for detection of bone metastases from breast cancer, it is apparent that it suffers from some limitations in depicting metastases of the osteoblastic type.

Keywords: FDG-PET – Bone metastases – Osteoblastic – Bone scintigraphy – Breast cancer

Eur J Nucl Med Mol Imaging (2005) 32:1253–1258
DOI 10.1007/s00259-005-1842-8

Introduction

Bone scintigraphy has been widely used to search for bone metastases, and it is undoubtedly useful because it permits a single whole-body examination with comparatively high sensitivity [1, 2]. However, in some instances it exhibits the disadvantage of low specificity and produces false positives due to uptake by benign lesions, such as osteoarthritis, fractures and inflammation; consequently even experienced nuclear physicians often have difficulty in distinguishing bone metastases from benign disease.

2-[¹⁸F]-Fluoro-2-deoxy-D-glucose positron emission tomography (FDG-PET) is useful for staging cancers, detecting recurrences and evaluating the effectiveness of treatment, and it has been reported to be of particular value when searching for bone metastases from breast cancer [3, 4]. Accordingly, for the latter purpose we expected FDG-PET, which reflects glucose metabolism in tumours, to be more sensitive than bone scintigraphy, which detects reactive bone metabolism. However, in our clinical routine we have encountered patients with no FDG uptake in whom computed tomography (CT) has clearly demon-

An editorial commentary on this paper is available at <http://dx.doi.org/10.1007/s00259-005-1869-x>

Takako Nakai (✉)
Department of Radiology,
Kyoto Prefectural University of Medicine,
465 Kajicho Kawaramachi-Hirokouji Kamigyō Kyoto,
Kyoto, 602-8566, Japan
e-mail: tootuka@koto.kpu-m.ac.jp
Tel.: +81-75-2515620, Fax: +81-75-2515840

Table 1. Comparison of the sensitivity, specificity and accuracy of bone scintigraphy and FDG-PET for the detection of bone metastases

	Sensitivity	Specificity	Accuracy
Bone scintigraphy	78.2 (43/55)	82.4 (28/34)	79.8 (71/89)
FDG-PET	80.0 (44/55)	88.2 (30/34)	83.1 (74/89)

The test showed no significant differences

strated osteoblastic metastases, which also typically displayed abnormal accumulation on bone scintigraphy. In previous studies, low rates of detection of osteoblastic metastases from prostate and breast cancers using FDG-PET have been described [5, 6]. In this study, we further extended the investigation by directly comparing FDG-PET and bone scintigraphy for the detection of bone metastases from breast cancer. Each bone lesion was classified as being of blastic, lytic, mixed or invisible type on the basis of the CT findings. By comparing the differences in accumulation between bone scintigraphy and FDG-PET, we attempted to clarify the pitfalls of using FDG-PET for the detection of osteoblastic bone metastases.

Materials and methods

Patients

The subjects were 89 breast cancer patients who had been treated in our hospital between September 2003 and December 2004. They ranged in age from 29 to 83 years, and their mean age was 59±15 years. Based on the biopsy and magnetic resonance imaging (MRI) findings and the clinical course, bone metastases were definitively diagnosed in a total of 55 patients. MRI studies were performed in all 55 patients with bone metastases, and 51 of the 55 patients had evidence of progressive metastatic disease during the study period or

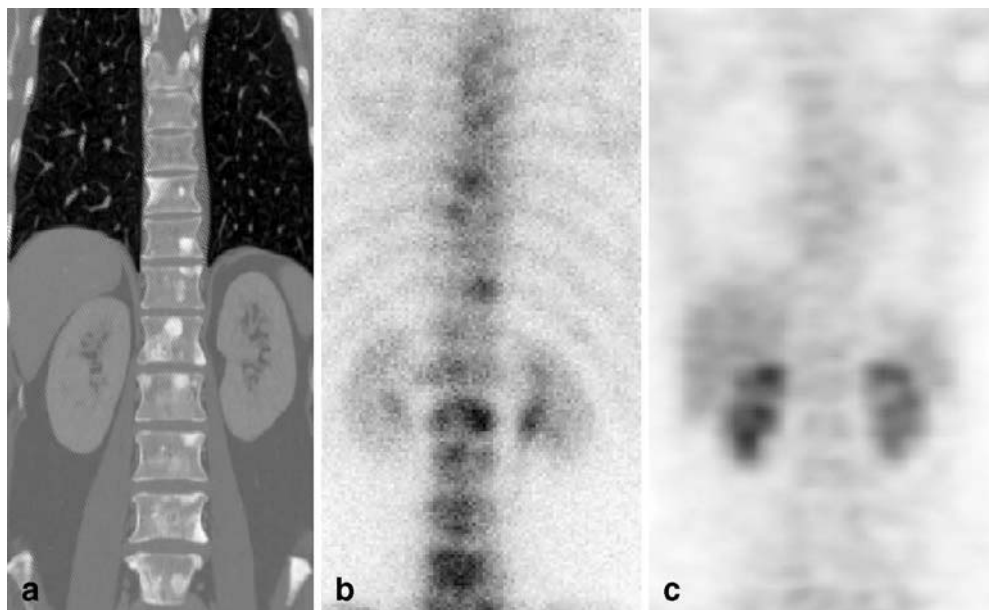
improvement following treatment. Histological confirmation was obtained in six patients. None of the 55 patients had previously received any treatment such as hormone manipulation therapy, chemotherapy or radiotherapy to the bone lesions. All patients provided written informed consent before entry into the study.

Imaging

All patients underwent bone scintigraphy and FDG-PET within 4 weeks of each other (mean interval 2.5 weeks). For bone scintigraphy, 740 MBq (20 mCi) of ^{99m}Tc-hydroxymethylene diphosphonate (HMDP) (Nihon Medi-Physics Co., Ltd.) was intravenously injected, and planar anterior and posterior images were obtained 2 h later. Single-photon emission computed tomography (SPECT) imaging of sites of suspected bone lesions was also performed in all patients. A dual-headed gamma camera, PRISM 2000XP (Royal Philips Electronics, Cleveland, USA), equipped with a low-energy high-resolution collimator, was used. After a 4-h fast, patients were intravenously injected with approximately 250–300 MBq (body weight × 5 MBq) of ¹⁸F-FDG. Fifty minutes after the injection, the patient voided, and 60 min after the injection, 23-s transmission scans and 2.5-min emission scans were obtained from the upper thigh to the neck using a dedicated high-resolution system (Allegro; Philips/ADAC, Cleveland, USA) with a 56-cm axial field of view, a resolution of 5.1 mm (axial) × 6.2 mm (in-plane) full-width at half-maximum, and a three-dimensional acquisition mode. The acquisition data were reconstructed by segmented attenuation correction and a three-dimensional raw action maximum likelihood algorithm (3D-RAMLA) method.

The degree of osteosclerosis and osteolysis in metastatic bone lesions was evaluated on the images obtained by 16-detector multislice CT (Aquilion, Toshiba Medical Systems Corp, Nasu, Japan). Multislice CT imaging of sites of bone metastases was performed using the following scanning parameters: rotation time, 0.5 s; detector collimation, 16×1 mm; voltage, 120 kV; amperage, 250–300 mA; and pitch, 15/16. Bone metastases on axial, sagittal and coronal images on a bone window (window width 2,200/window level 200) were visually classified into four types: blastic, lytic, mixed and invisible. Metastases were classified as being of the invisible type when there was no difference in appearance compared with surrounding normal bone.

Fig. 1. **a** Coronal CT image of multiple blastic-type bone metastases in a 75-year-old-woman after surgery for breast cancer. Sclerotic changes were seen in multiple vertebral bodies. **b** Posterior bone scintigram. Uptake was observed in multiple vertebral bodies. **c** Coronal FDG-PET image. No uptake is seen in the bone metastases



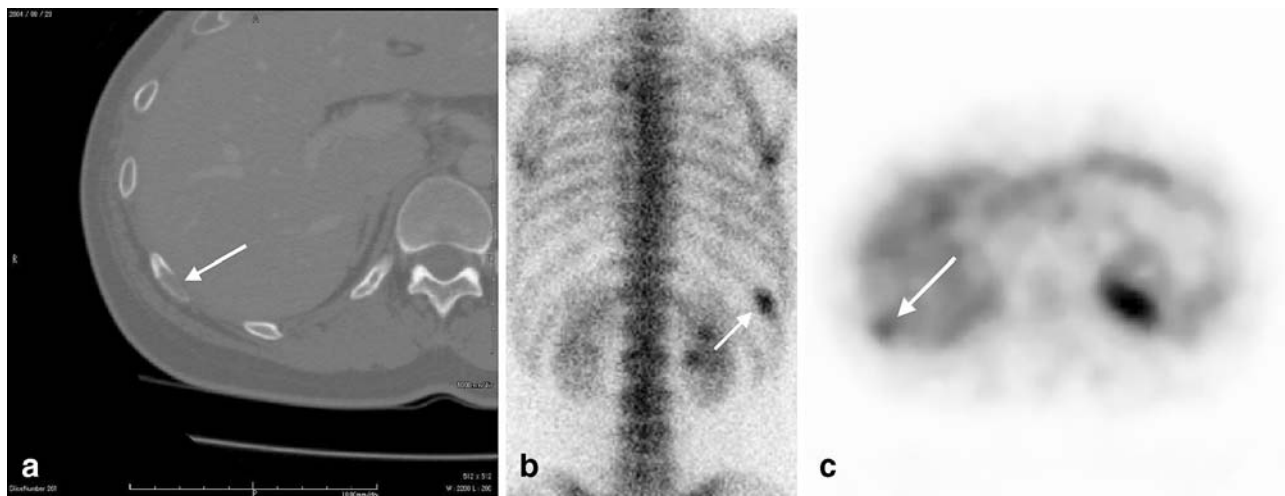


Fig. 2. **a** Axial CT image of a lytic-type metastasis in a 75-year-old man with breast carcinoma. A lytic metastasis is visible in the right 10th rib (*arrow*). **b** Posterior bone scintigram. The 10th rib contains a lytic metastasis in the form of a hot lesion (*arrow*), highly suggestive of a metastasis. **c** Axial FDG-PET image. Uptake was observed in the lytic metastasis to the 10th rib (*arrow*)

The sensitivity, specificity and accuracy of FDG-PET and bone scintigraphy were calculated on a patient by patient basis for each type. The mean standard uptake values (SUV_{mean}) of the four types of bone metastasis on FDG-PET were measured and compared. FDG-PET, bone scintigraphy and CT images were evaluated independently by two board-certified nuclear physicians.

Statistical analysis

The results of FDG-PET and bone scintigraphy were compared using the McNemar test. P values <0.05 were considered significant.

Fig. 3. **a** Axial CT image of a mixed-type metastasis in a 49-year-old woman after surgery for breast cancer. A mixed blastic-lytic metastasis is seen in the vertebral body of T7 (*arrow*). **b** Posterior whole-body bone scintigram. High uptake is seen in the vertebral body of T7 (*arrow*). Multiple bone metastases were suspected because of the presence of uptake in the right 5th and 8th ribs, suggestive of metastases. **c** Axial FDG-PET image. FDG-PET showed high uptake in T7 (*arrow*), corresponding to the uptake on bone scintigraphy

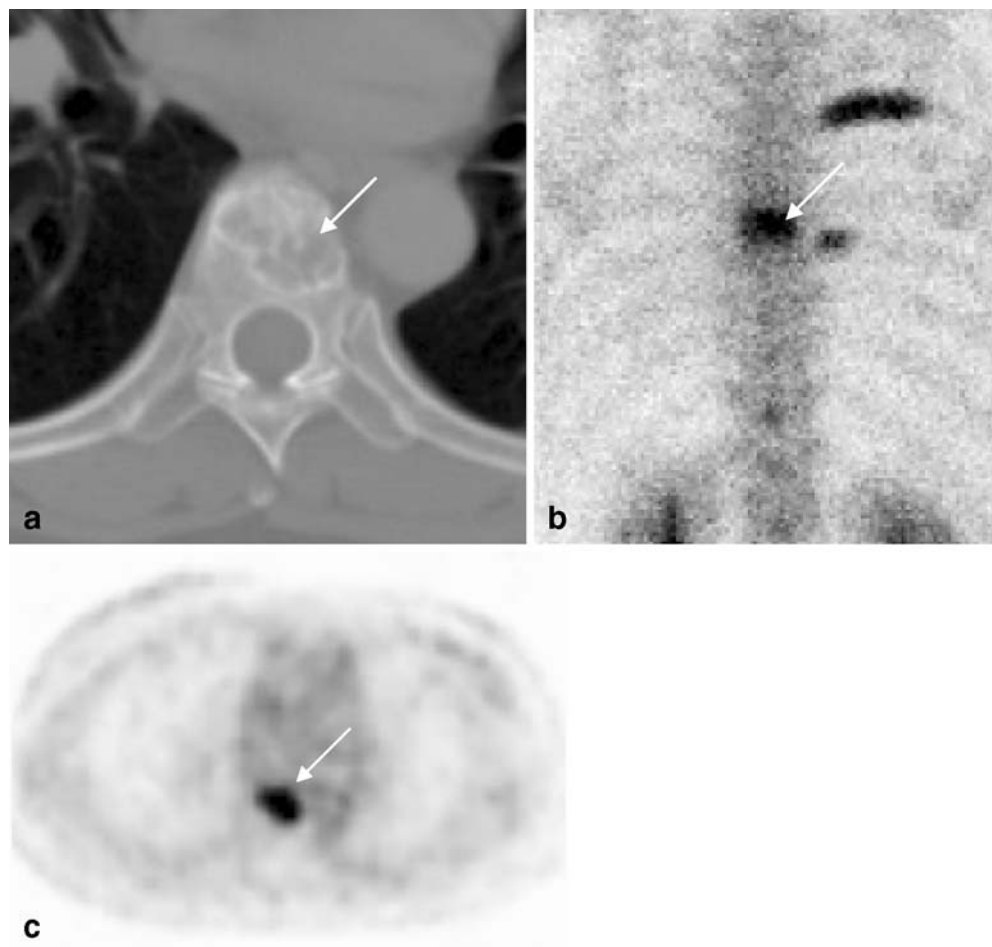
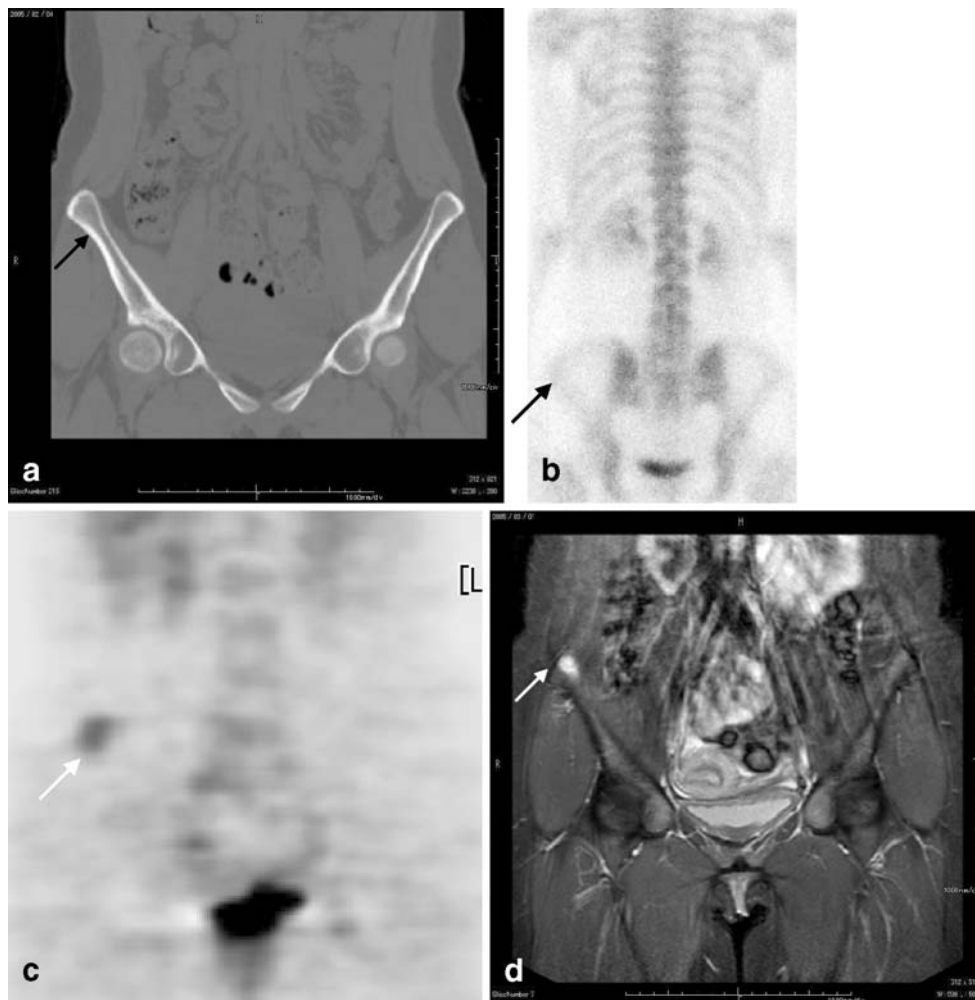


Fig. 4. **a** Coronal CT image of an invisible metastasis in a 55-year-old woman after surgery for breast cancer. The metastasis should be present at the site indicated by the *arrow*, but could not be clearly seen. **b** Posterior bone scintigrams. Uptake in the ilium bone metastasis is unclear (*arrow*). **c** Coronal FDG-PET image. Uptake was seen in the ilium (*arrow*). This metastasis had a SUV_{mean} of 2.9. **d** Gadolinium-enhanced MR image with coronal fat suppression. Enhanced signal intensity is seen in the ilium (*arrow*), suggesting a bone metastasis. The lesion grew larger during follow-up, suggesting bone metastases clinically



Results

Bone metastases were present in 55 patients. Bone scintigraphy revealed ^{99m}Tc -HMDP uptake at 49 sites that were diagnosed as metastases, but was false positive at six sites and false negative at 12 sites. FDG-PET revealed FDG uptake at 48 sites, but it was false positive at four sites and false negative at 11 sites. The causes of the false positives on bone scintigraphy were a rib or sternal traumatic fracture, osteoarthritis of a vertebral body, osteomyelitis and a bone island. The false positives on FDG-PET were due to a rib fracture or acute coxitis.

Table 2. The visualisation rates of bone scintigraphy and FDG-PET for the different CT types of bone metastases

CT type	Bone scintigraphy	FDG-PET	<i>p</i> value
Blastic (18)	100.0 (18/18)	55.6 (10/18)	<i>p</i> <0.0781
Lytic (10)	70.0 (7/10)	100.0 (10/10)	NS
Mixed (19)	84.2 (16/19)	94.7 (18/19)	NS
Invisible (8)	25.0 (2/8)	87.5 (7/8)	<i>p</i> <0.0313

NS=significant

The sensitivity, specificity and accuracy of bone scintigraphy were 78.2%, 82.4% and 79.8% respectively, and the corresponding values for FDG-PET were 80.0%, 88.2% and 83.1%, respectively. The sensitivity, specificity and

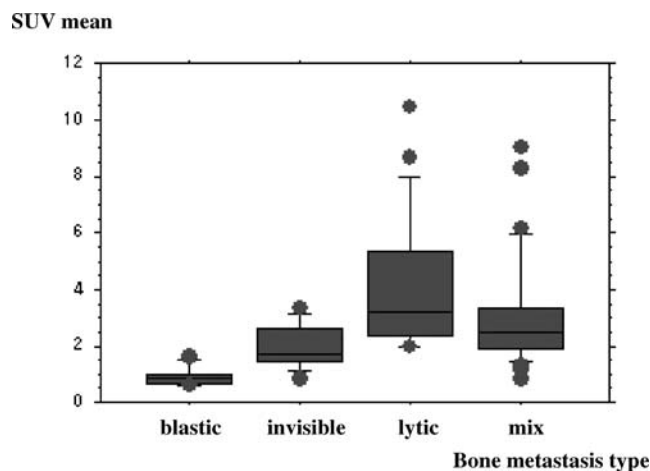


Fig. 5. Box-whisker graph of SUV_{mean} values of the different types of bone metastases

accuracy of FDG-PET were higher, but the difference was not significant (Table 1).

Bone metastases were classified on CT as being of the blastic, lytic, mixed and invisible types at 18, 10, 19 and 8 sites, respectively. Representative CT patterns are shown in Figs. 1, 2, 3 and 4. The visualisation rates of bone scintigraphy and FDG-PET for the four types are shown in Table 2. The visualisation rate of FDG-PET for the blastic type (55.6%, 10/18) was significantly lower than that of bone scintigraphy ($p < 0.0781$). The visualisation rate of FDG-PET for the invisible type (7/8) was significantly higher than that of bone scintigraphy ($p < 0.0313$). There was no significant difference in the visualisation rates of the two imaging modalities for the lytic and mixed types.

The SUV_{mean} values of the blastic, lytic, mixed and invisible types were 1.72 ± 0.28 , 4.14 ± 2.20 , 2.97 ± 1.98 and 2.25 ± 0.80 , respectively. The SUV_{mean} of the lytic type tended to be higher than that of the blastic type, and the SUV_{mean} values of the mixed and invisible types were intermediate between those of the blastic type and the lytic type (Fig. 5).

Discussion

FDG-PET has been shown to be superior to bone scintigraphy for the detection of bone metastases [2–5]. This is in keeping with the results of our study, which showed a general trend towards a higher rate of lesion detection using FDG-PET. The rate of visualisation of osteoblastic metastases, however, was significantly higher with bone scintigraphy than with FDG-PET. On bone scintigraphy, increased accumulation in blastic metastases is usually observed owing to an osteoblastic bone reaction to cancer cells; however, the cause of the decreased FDG uptake by osteoblastic bone metastases on FDG-PET is largely unknown [5]. According to the mechanisms of bone metastasis proposed by Galasko et al., bone formation and destruction occur simultaneously, but, in blastic metastases, bone formation by osteoclasts predominates in the space that results after bone destruction, whereas in lytic metastases, bone destruction and tumour cell growth predominate in the bone resorption space, and mixed metastases represent a mixture of blastic and lytic metastases [6]. Based on these mechanisms of bone metastasis, we postulated that the decreased FDG uptake in blastic bone metastases may be explained as follows: osteoblast proliferation in blastic metastases results in an increase in the bone matrix and a relative decrease in cell density; this leads to lower FDG accumulation since FDG uptake in tissue reflects the underlying glucose metabolism and cell density.

Another factor to be considered is the degree of malignancy. Shreve et al. ascribed the low SUVs on FDG PET for osteoblastic metastases, including those from prostate cancer, to the low malignancy of the primary lesion [7]. This theory can be extrapolated to bone metastases from breast cancers, and the degree of aggres-

siveness of the primary lesion may have had a direct relationship with the SUVs in our population, too. In fact, Cook et al. reported that osteoblastic metastases of breast cancer with low FDG uptake had a good outcome, whereas their osteolytic counterparts with high FDG uptake had a poor outcome [8].

The visualisation rate of FDG-PET for lytic metastases was high (100.0%). Since breast cancer cells with very rapid glucose metabolism grow in the resorption space in osteolytic metastases, high FDG uptake can be easily predicted, and osteolytic metastases are frequently associated with extraosseous mass formation, resulting in a higher detection rate. Presumably the uptake of FDG by mixed (blastic–lytic) metastases will depend on the balance between decreased uptake by blastic metastases and increased uptake by lytic metastases.

The invisible-type metastases in our series of patients were devoid of bone destruction and also small, often less than 5 mm. We believe that the invisible type in our study corresponds pathologically to the intertrabecular type of bone marrow metastasis described by Yamaguchi et al. In their study, these lesions were characterised by tumour cell infiltration of the bone marrow space without apparent bone destruction. Yamaguchi et al. pointed out that radiographs and scintigraphy often failed to show any findings in lesions with the intertrabecular pattern [9]. Intertrabecular metastases are frequently minute metastatic lesions 2–3 mm in diameter, and it has been reported that early-stage metastases detected on imaging studies are often of the intertrabecular type [10]. An animal experiment by Hiraga et al. showed that intertrabecular type metastases are characterised by rapid tumour cell growth, scant stroma around the tumour cells and fewer osteoclasts than are present in normal bone [11], suggesting that scant deposition of hydroxyapatite-containing matrix results in the absence of increased uptake. The visualisation rate of bone scintigraphy for isodensity-type metastases in the present study (25%) was very low, indicating that many bone metastases not visualised by multislice CT are also not visualised by bone scintigraphy. The visualisation rate of FDG-PET for invisible type metastases, on the other hand, was higher than expected, suggesting that FDG-PET may contribute to the detection of microscopic early bone marrow metastases that are too small to be visualised by bone scintigraphy or multislice CT. This may be because invisible-type bone metastases grow rapidly and have rapid glucose metabolism.

Although osteoarthritis was among the causes of false-positive results on bone scintigraphy, FDG-PET yielded true-negative results in patients with osteoarthritis, which increased its specificity. We speculate that glucose metabolism is not very rapid in osteoarthritis, except in the acute stage. However, since FDG-PET produces false-positive results in lesions in which glucose metabolism is predicted to be rapid, such as acute osteomyelitis and fractures [12, 13], images should be carefully interpreted in conjunction with consideration of symptoms and clinical findings.

Conclusion

FDG-PET was shown to be useful in detecting bone metastases from breast cancer. It does, however, suffer from the drawback of a lower visualisation rate for osteoblastic bone metastases, presumably because of the low density of cells embedded in the bone matrix and the absorption of radioactivity. Care must be taken when using FDG-PET alone to search for bone metastases in breast cancer patients.

References

1. Merrick MV. Review article—bone scanning. *Br J Radiol* 1975;48(569):327–51
2. Bury T, Barreto A, Daenen F, Barthelemy N, Ghaye B, Rigo P, et al. Fluorine-18 deoxyglucose positron emission tomography for the detection of bone metastases in patients with non-small cell lung cancer. *Eur J Nucl Med* 1998;25:1244–7
3. Bender H, Kirst J, Palmedo H, Schomburg A, Wagner U, Ruhlmann J, et al. Value of 18fluoro-deoxyglucose positron emission tomography in the staging of recurrent breast carcinoma. *Anticancer Res* 1997;17:1687–92
4. Ohta M, Tokuda Y, Suzuki Y, Kubota M, Makuuchi H, Tajima T, et al. Whole body PET for the evaluation of bony metastases in patients with breast cancer: comparison with ^{99m}Tc^m-MDP bone scintigraphy. *Nucl Med Commun* 2001;22:875–9
5. Peterson JJ, Kransdorf MJ, O'Connor MI. Diagnosis of occult bone metastases: positron emission tomography. *Clin Orthop* 2003;(415 Suppl):S120–8
6. Galasko CS. Mechanisms of lytic and blastic metastatic disease of bone. *Clin Orthop* 1982;169:20–7
7. Shreve PD, Grossman HB, Gross MD, Wahl RL. Metastatic prostate cancer: initial findings of PET with 2-deoxy-2-[F-18] fluoro-D-glucose. *Radiology* 1996;199(3):751–6
8. Cook GJ, Houston S, Rubens R, Maisey MN, Fogelman I. Detection of bone metastases in breast cancer by ¹⁸F¹⁸FDG PET: differing metabolic activity in osteoblastic and osteolytic lesions. *J Clin Oncol* 1998;16(10):3375–9
9. Yamaguchi T, Tamai K, Yamato M, Honma K, Ueda Y, Saotome K. Intertrabecular pattern of tumors metastatic to bone. *Cancer* 1996;78(7):1388–94
10. Moriwaki A, Manny K. Bone marrow metastasis in autopsy cases: histopathologic features from early metastasis to advanced stage. *Gan No Rinsyo* 2003;49:35–42
11. Hiraga T, Ozawa H. Microstructure of bone metastasis. *Byori to Rinsho* 1999;17:35–38
12. Shon IH, Fogelman I. F-18 FDG positron emission tomography and benign fractures. *Clin Nucl Med* 2003;28:171–5
13. Ravenel JG, Gordon LL, Pope TL, Reed CE. FDG-PET uptake in occult acute pelvic fracture. *Skelet Radiol* 2004;33:99–101